PROCEEDINGS OF SCIENCE

Modeling flat proton spectra at large solar energetic particle events at 1 AU via particle escape into a self-generated/pre-existing turbulence

Federico Fraschetti[a,b,*] **and Greta R. Goldberg**[c,d]

[a] *Center for Astrophysics | Harvard & Smithsonian, 60 Garden Street, Cambridge MA 02138, USA*
[b] *Department of Planetary Sciences - Lunar and Planetary Lab, Tucson, AZ, 85721*
[c] *NYU Department of Physics - 726 Broadway, New York, NY 10003 USA*
[d] *ATLAS Experiment, CERN CH-1211 Geneva 23 Switzerland*

E-mail: federico.fraschetti@cfa.harvard.edu

Flat proton energy (50 keV – a few MeV) spectra have been measured in-situ at 1 AU in large solar energetic particle events in the past decades. The diffusive picture of particle acceleration at shocks propagating into media that enforce a uniform spatial diffusion far upstream (several hours at 1 AU) seems unable to reproduce such measurements. Hereby we use a method recently developed based on a 1D transport equation accounting for particle acceleration and escape, both allowed at all particle energies, not only the highest energies. The key ingredient of the model is that diffusion is contributed by both self-generated turbulence close to the shock and by pre-existing turbulence far upstream, so that the upstream mean free path gradually increases out to a saturation in the pristine solar wind turbulence. The steady-state spectra agree very well with in-situ measurements, confirming that escape into a medium with mean free path spatial variation is a crucial ingredient in forging the energy spectra in the proximity of shocks.

38th International Cosmic Ray Conference (ICRC2023)
26 July - 3 August, 2023
Nagoya, Japan

*Speaker

PoS(ICRC2023)1317

1. Introduction

Recently measured proton spectra of large SEP events at interplanetary shocks at 1 AU have shown [1] an unprecedentedly flat shape over the energy range (50 keV – a few MeV), in tension with decades of in-situ measurements and with the current models.

One of the first models for the particle acceleration at shocks in the presence of self-excited waves [2] already predicted an upstream softening of the energy spectrum. The reason lies in the enhanced fluctuations that enable more efficient confinement at the shock of low energy than of high energy particles; thus, the intensity of the former in the upstream medium is depleted, resulting in flatter spectrum [see also the review 3]. However, it is not clear whether the nearly zero spectral slope measured by [1] could be reached in a particular scattering condition. A more recent modeling attempt for the SEP events reported in [1] also suggests trapping of low energy particles as origin of upstream spectral flatness [4].

In this paper we report the application to 4 flat spectra events at 1 AU of a 1-D model recently presented [5] for the acceleration and escape of energetic particles at shocks. The in-situ measured shock parameters are directly used to fit energetic particles data of each individual shock event.

2. Observations

Recently, a number of large SEP events preceding the passage of interplanetary shocks were reported to exhibit a 12 – 24 hours time interval with an in-situ measured flat energy spectrum [1]. In particular, the Low-Energy Magnetic Spectrometer (LEMS120) telescope onboard the Advanced Composition Explorer (ACE) measured ions flux in the range $47 - 4,800$ keV and the detector telescope SST-O of the Three-Dimensional Plasma and Energetic Particle Investigation (3DP) onboard Wind spacecraft measured ions flux from a few tens of keV up to 11 MeV. The sample in [1] includes 11 events.

In this work we focus on the 4 ACE shock crossings. The shock parameters reported in [1] and herein used for the fit of energy spectrum and intensity profile, after average over a longer time-interval, are listed in table 1.

Shock Date	U_1 (km/s)	r	V_{sh} (km/s)
5/15/2005	356.49 ± 85.85	5.74 ± 1.42	469.60
11/4/2003	251.02 ± 710.00	3.83 ± 1.03	536.06
4/28/2001	525.72 ± 104.62	2.20 ± 0.43	437.78
9/15/2000	111.18 ± 39.00	2.21 ± 0.28	383.69

Table 1: Measured parameters of the 4 ACE/EPAM shocks from [1].

Here U_1 is the shock speed in the upstream plasma frame averaged over a 9-minutes interval before the shock arrival[1], r the density compression and V_{sh} is the shock speed in spacecraft frame averaged over the flat spectrum time interval by using time-series from the ACE Science Center[2].

[1] http://ipshocks.fi/database

[2] https://izw1.caltech.edu/ACE/ASC/level2/index.html

Ion species are not distinguished by these telescopes. We will assume that intensities measured by both instruments are dominated by protons and the contribution of alpha particles and heavy ions is small compared to that of protons.

A striking and yet unexplained feature of the flat spectra is the variable time-lag to the shock: in some cases such time interval extends until < 30 minutes before the shock passage whereas in other cases it ends several hours before the shock and the later spectrum steepens close to the diffusive shock acceleration (DSA) prediction. This set of measurements suggests that, at least in cases of small time-lag, the spectrum at the shock itself can be flatter than DSA if the diffusion is strongly enhanced therein.

3. Outline of the model

In order to explain the ACE measurements we use the 1-D model of transport proposed in [5] that combines in a single spatial diffusion coefficient the effect of pre-existing turbulence far upstream from the shock and the self-excited fluctuations. This model also introduces a spatially and energy-dependent escape time $T(x,p)$ that describes the escape of energized particles from the shock at all energies, not just the energies beyond a given cutoff, and at all distances from the shock, not only at a free escape boundary. This model was extended to the case of a source term given by a power-law momentum distribution [6]. This model also provided an excellent fit of all of the Ground Level Enhancements (GLEs) of solar cyle 23 [7].

For an infinitely planar shock wave the 1-D steady-state transport equation for the phase-space distribution function for the energetic particles $f(x,p)$, is recast, assuming pitch-angle isotropy in the local plasma frame, as [5]:

$$U\frac{\partial f(x,p)}{\partial x} = \frac{\partial}{\partial x}\left[\kappa(x,p)\frac{\partial}{\partial x}f(x,p)\right] + \frac{1}{3}\left(\frac{dU}{dx}\right) p \frac{\partial f(x,p)}{\partial p} + S(x,p) - \frac{f(x,p)}{T(x,p)}, \qquad (1)$$

where the flow speed is written as:

$$U = \begin{cases} U_1 & \text{if } x < 0, \text{upstream} \\ U_2 & \text{if } x > 0, \text{downstream}\,. \end{cases}$$

The upstream diffusion is contributed by both pre-existing turbulence far from the shock and by self-generated turbulence closer to it. The latter dominates out to a distance $|x| = \Lambda_1$, where the pre-existing fluctuations inherent to the interplanetary/interstellar medium [8] take over. The catastrophic loss term $f(x,p)/T(x,p)$ represents the escape from the shock with a time scale $T(x,p)$; if $T(x,p)$ becomes much greater than the acceleration time scale, the solution collapses to the no-escape DSA solution. The energy-dependent $T(x,p)$ replaces the energy-independent free escape boundary, location far upstream assumed in numerical simulations to represent the boundary of particle propagation in scatter-free regime [5].

For simplicity, a separable κ is assumed:

$$\kappa(x,p) = \begin{cases} \kappa_1(p)\frac{|x-\epsilon|}{|\Lambda_1|} & \text{if } x < 0 \text{ and } |x| < |\Lambda_1|, \text{upstream} \\ \kappa_1(p) & \text{if } x < 0 \text{ and } |x| > |\Lambda_1|, \text{far upstream} \\ \kappa_2(p) & \text{if } x > 0, \text{downstream}\,, \end{cases} \qquad (2)$$

where $\kappa_i(p)$ depends only on momentum and $i = 1, 2$ indicates respectively upstream and downstream, $\epsilon = d_i \simeq 10^7$ cm is the ion inertial length, approximate thickness of the shock transition layer [9]. Here $\kappa \rightarrow \kappa_1(p)$ as $x \rightarrow \Lambda_1$ is the far upstream diffusion coefficient in the pre-existing turbulence. Since the upstream T is expected to decrease with the distance from the shock due to the smaller density of scattering centers, the escape time is recast as

$$T(x,p) = \begin{cases} T_1(p)\frac{|\Lambda_1|}{|x-\epsilon|} & \text{if } x < 0 \text{ and } |x| < |\Lambda_1|, \text{upstream} \\ T_1(p) & \text{if } x < 0 \text{ and } |x| > |\Lambda_1|, \text{far upstream} \\ T_2(p) & \text{if } x > 0, \text{downstream.} \end{cases} \tag{3}$$

We assume a monochromatic source localized at the shock: $S(x,p) = S_0\delta(x)\delta(p-p_0)$ and a power-law p-dependence of κ and T:

$$\kappa_i(p) = \bar{\kappa}_i(p/p_0)^{\delta_i}, \quad T_i(p) = \bar{T}_i(p/p_0)^{-\gamma_i}, \quad \delta_1 > \gamma_1 \tag{4}$$

where $\bar{\kappa}_1 = \kappa_1(\Lambda_1, p_0)$, $\bar{\kappa}_2 = \kappa_2(p_0)$, $\bar{T}_1 = T_1(\Lambda_1, p_0)$, $\bar{T}_2 = T_2(p_0)$ and power-law indexes $\delta_i > 0$, $\gamma_i > 0$.

4. Modeling flat energy spectra at 1 AU

In order to compare the model [5] to in-situ measurements, we first fitted the energy spectra of the 4 ACE events listed in table 1 throughout the ACE/EPAM/LEMS120 energy bands (47 keV - 4.8 MeV) or, for 3 events, over the 7 highest energy bands of the 8 available. Assuming both spatially-dependent upstream escape time $T_1(x,p)$ and spatial diffusion coefficient $\kappa_1(x,p)$ (see Eq.s 2 and 3), we applied to ACE data the following expression for the momentum spectrum [at the shock, 5]

$$f(E) \propto \left(\frac{E}{E_0}\right)^{-\frac{q}{2}} \exp\left[-A_1\left(\frac{E}{E_0}\right)^{-\frac{\delta_1}{2}}\right] \exp\left[-A_2\left(\frac{E}{E_0}\right)^{\frac{\delta_2+\gamma_2}{2}}\right] \tag{5}$$

where we have assumed an injection energy $E_0 = 100$ keV for all 4 events, $q = 3r/(r-1)$ is the DSA test-particle power law in the case of no-escape and

$$A_1 = 0.4\,\frac{q}{\delta_1}\,\frac{U_1}{400\,\mathrm{km/s}}\,\frac{|\Lambda_1|}{10^{11}\,\mathrm{cm}}\left(\frac{\bar{\kappa}_1}{10^{19}\,\mathrm{cm^2/s}}\right)^{-1}\left|-5.3+\log\frac{\epsilon/10^7\mathrm{cm}}{L_1(E_0)/10^9\mathrm{cm}}\right|, \tag{6}$$

$$A_2 = 6.25\times10^{-5}\,\frac{q}{r(\delta_2+\gamma_2)}\,\frac{\bar{\kappa}_2}{10^{15}\,\mathrm{cm^2/s}}\left(\frac{U_2}{400\,\mathrm{km/s}}\right)^{-2}\left(\frac{\bar{T}_2}{10^4\,\mathrm{sec}}\right)^{-1} \tag{7}$$

where we have used the continuity conditions at the shock $\bar{\kappa}_2 = \kappa_1(0,E_0)$ and $\bar{T}_2 = T_1(0,E_0)$. The upstream escape length $L_1(E_0) = \sqrt{\kappa_1(x,E_0)T_1(x,E_0)} = \sqrt{\kappa_1(0,E_0)T_1(0,E_0)}$, independent on position x, was shown in [5] to take the role of the diffusion length in the DSA model in determining the steepness of the upstream intensity profile of the energetic particles.

In the fit of the energy spectra, the measured shock compression ratios as reported in the Heliospheric Shock Database[3] and the measured shock speeds as reported in the ACE database[4] were

[3] https://ipshocks.fi/database

[4] https://izw1.caltech.edu/ACE/ASC/level2/index.html

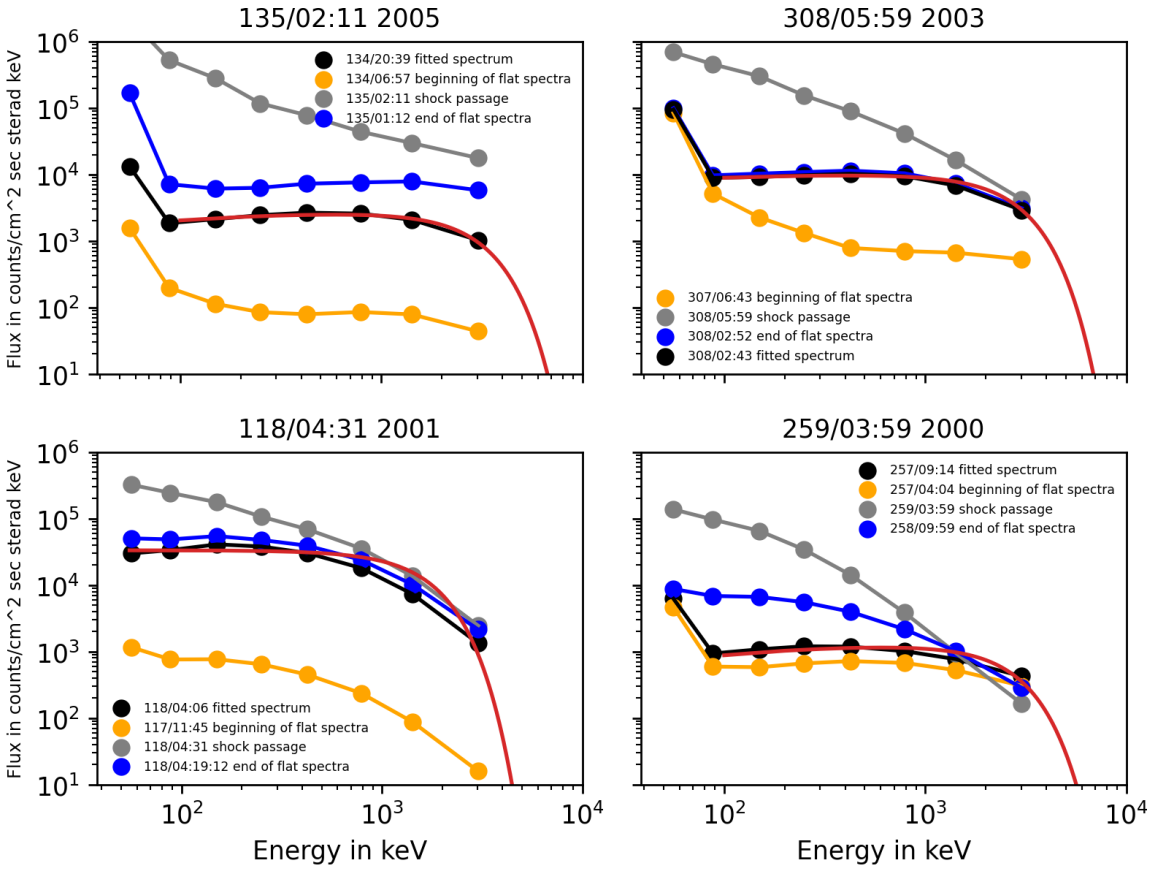

Figure 1: Energy spectra for four distinct shocks compared with the model [5] in Eq. 5. Each dataset (in black) fitted by the model curve (in red) corresponds to an arbitrarily selected time between the beginning/end of the flat spectrum time interval, respectively in dark yellow/blue. The spectrum at the shock passage is shown in grey. The fit of spectra of years 2005, 2003, and 2000 shocks is based on the 7 highest-energy of the 8 ACE/EPAM/LEMS120 energy bands due to the possible contamination of the thermal part of the spectrum in the far unshocked medium.

used. In the fitting procedure of the spectra, the escape timescale T, the spatial diffusion coefficient κ and the length scale Λ_1 are the model parameters independently varied (see table 2).

Shock Date	$\bar{\kappa_1}$ (cm^2/s)	$\bar{T_1}$ (s)	Λ_1 (cm)	Λ_1/V_{sh} (s)
5/15/2005	2.3×10^{18}	870	3×10^{11}	6.4×10^3
11/4/2003	3.5×10^{18}	1700	3×10^{11}	5.6×10^3
4/28/2001	3.35×10^{19}	1000	2×10^{11}	4.6×10^3
9/15/2000	3.5×10^{19}	5300	2.85×10^{12}	7.4×10^4

Table 2: Model parameters from the preliminary best-fit of energy spectra and intensity profiles for the 4 ACE shocks listed in table 1; here, $\bar{\kappa_1}$ and $\bar{T_1}$ are defined in Eq. 4.

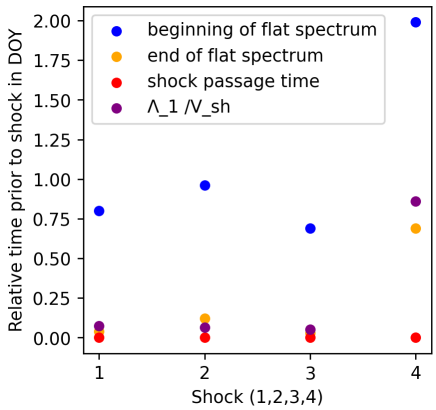

Figure 2: Instants of time as fraction of day at the spacecraft for each shock relative to the shock passage representing the beginning/end of the flat spectrum interval (blue/dark yellow), shock arrival (red) and the value of Λ_1/V_{sh} (black). The labels 1, 2, 3, 4 are associated with the shock on DOY 135 of 2005, on DOY 308 of 2003, on DOY 118 of 2001, on DOY 259 of 2000, respectively.

Figure 1 shows the fit of the in-situ measurements, spectra at the beginning/end of the flat spectrum interval and the spectra at the shock arrival. The best-fit parameter set is shown in table 2. From Eq.s 2 and 3, the far upstream values $\bar{\kappa}_1$ and $\bar{T}_1$, for $E = E_0$, correspond to values at the shock $\kappa_1(10\,\epsilon, E_0) \sim 10^{15}$ cm^2/s and $T_1(10\,\epsilon, E_0) = 10^6$ sec, longer than the shock lifetime (where $10\,\epsilon$ incorporates the shock transition layer); in other words, the escape at energy as low as $E = E_0$ is forbidden. An important caveat is that the model in Eq. 5 provides the spectrum at the shock but Fig.1 shows that the measured spectrum steepens between the end of the flat spectrum time interval and the shock. In this case we expect a tension between model, strictly valid at the shock, and data.

Figure 2 compares the times of the beginning/end of the flat spectrum time intervals with the advection time scale, in the spacecraft frame, of the region presumably dominated by the self-excited turbulence, i.e., Λ_1/V_{sh}. For shock 4 (DOY 2000/259), the $\sim$ 0.75 day time-lag between the end of the flat spectrum time interval and Λ_1/V_{sh} suggests that the spectrum is flattened by the turbulence pre-existing the shock arrival rather than the self-excited turbulence. In the cases 1, 2, 3, the advection scale Λ_1/V_{sh} nears by minutes the end of the flat spectrum time interval and the role of self-excited turbulence in flattening the spectrum cannot be ruled-out.

5. Modeling the upstream intensity profiles

Once the shock parameters are determined from the spectral fits (see Fig.1), the data for the upstream intensity profiles can be compared with the model prediction with no free parameters left (the downstream profile model is still underway).

The solution in position space x of Eq. 1, in the far upstream, i.e., for $|x - \epsilon| \gg L_1(p)$, can be recast as [5]

$$f(x,E) \rightarrow f_0(E)\,\frac{\Gamma(1-\nu_1)}{\sqrt{\pi}}\,\sin(\pi\nu_1)\,\left(\frac{|x-\epsilon|}{2L_1(E)}\right)^{\nu_1-1/2}\,\exp\left(-\frac{|x-\epsilon|}{L_1(E)}\right), \tag{8}$$

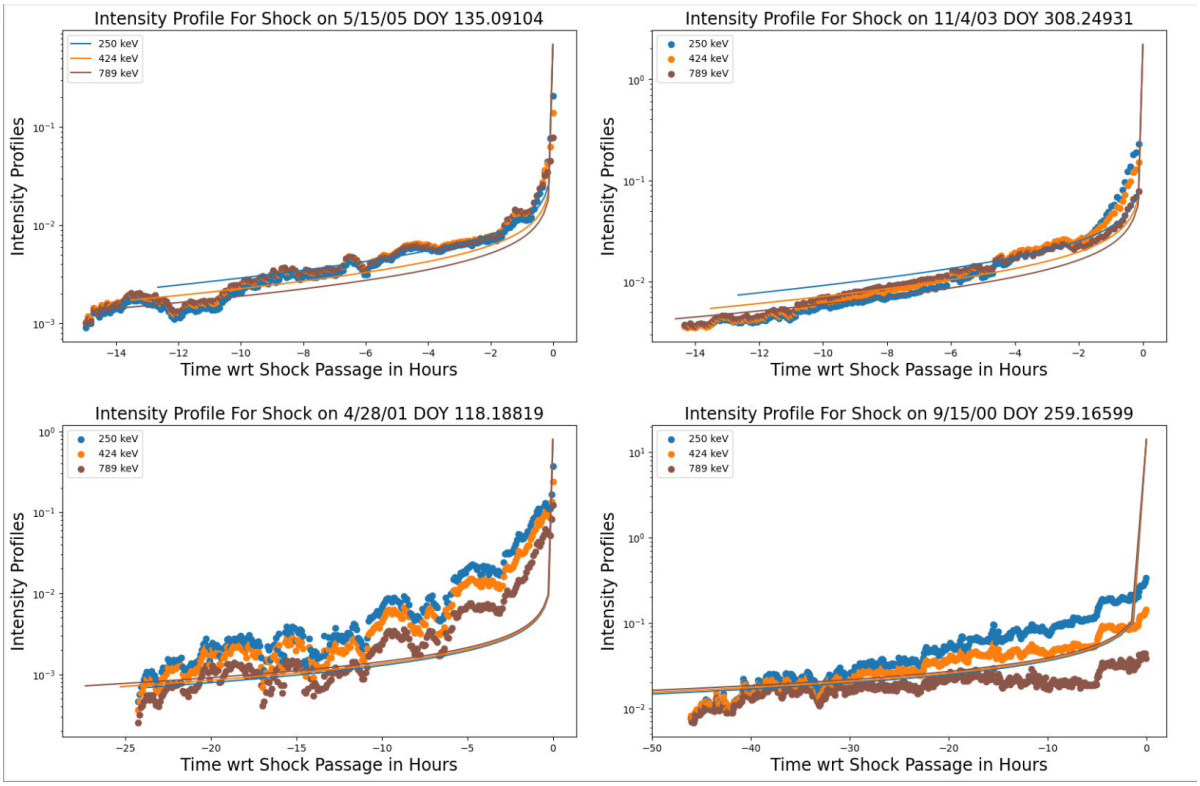

Figure 3: Upstream intensity profiles 5-minutes averaged in three selected energy bands with mean energy 250 (blue), 424 (orange) and 789 (brown) keV from ACE-EPAM/LEMS120, compared with the model prediction in Eq. 8. Data and model are normalized to the corresponding value of the mean energy 88 keV band within 12 seconds from the shock arrival. The model parameters determined from the energy spectra best-fit in Fig. 1 are here used, with no additional free parameters.

where $f_0(E)$ is the phase-space distribution function at the shock ($x = 0$) at a given energy E, $\Gamma(z)$ is the gamma function and $\nu_1(E) = |\Lambda_1|U_1/2\kappa_1(E)$. The far upstream profile is exponentially suppressed with roll-over scale $L_1(E)$ that replaces the diffusion scale $\sim \kappa_1(\epsilon, p)/U_1$, and further suppressed by the factor $(|x - \epsilon|/2L_1(E))^{\nu_1 - 1/2}$. Thus, particles do not disappear and still spread out to an infinite distance as in DSA, but with an amplitude smaller than DSA. The escape time $T_1(x, p)$ determines whether or not from a given upstream location and at a given energy particles come back to the shock. The fit of the intensity profiles of such a variety of cases with no free parameters is impressive.

6. Summary and Conclusions

We have presented a preliminary application of a 1-D model for particle acceleration and escape at shocks to 4 ACE shocks with a recently studied flat spectrum. The model parameters are determined from the spectral fit and with no additional free parameter upstream intensity profiles are compared with data. The upstream spectral flattening results from the trapping at low energy, already identified in the early versions of particle acceleration models [2], and escape at higher energies. The model here extended [5] seems to very satisfactorily account for spectral flatness

and intensity profiles. The strong variability of time lag between flat spectrum time interval and shock arrival (from a few minutes to 0.75 days) suggests that not only interplanetary turbulence can account for the efficient trapping of low energy particles but self-excited turbulence at the shock cannot be ruled out. Finally, the higher energy resolution and broader energy coverage of in-situ measurements by Parker Solar Probe and Solar Orbiter are likely to unveil several flat spectra events in the near future.

Acknowledgments

FF was supported, in part, by NSF under grant 1850774, by NASA under Grants 80NSSC18K1213, 80NSSC21K0119 and 80NSSC21K1766. Authors thank Mr. Thomas M. Do for help on Python visualization tools.

References

[1] D. Lario, L. Berger, I. Wilson, L. B., R.B. Decker, D.K. Haggerty, E.C. Roelof et al., *Flat Proton Spectra in Large Solar Energetic Particle Events*, in *Journal of Physics Conference Series*, vol. 1100 of *Journal of Physics Conference Series*, p. 012014, Oct., 2018, DOI.

[2] M.A. Lee, *Coupled hydromagnetic wave excitation and ion acceleration at interplanetary traveling shocks*, **88** (1983) 6109.

[3] D.V. Reames, *Particle acceleration at the Sun and in the heliosphere*, **90** (1999) 413.

[4] S. Perri, G. Prete, G. Zimbardo, D. Trotta, I. Wilson, Lynn B., D. Lario et al., *Interpretation of Flat Energy Spectra Upstream of Fast Interplanetary Shocks*, **950** (2023) 62 [2301.05454].

[5] F. Fraschetti, *Effect of Acceleration and Escape of Energetic Particles on Spectral Steepening at Shocks*, **909** (2021) 42 [2012.12073].

[6] T. Do, F. Fraschetti and M. Singh, *Model for the Energetic Particles Spectrum at Interplanetary Shocks resulting from Acceleration and Escape sourced by a Preexisting Population with Power Law Energy Spectrum*, in *AGU Fall Meeting Abstracts*, vol. 2021, pp. SH23C–03, Dec., 2021.

[7] F. Fraschetti and A. Balkanski, *Imbalance acceleration/escape of energetic particles at interplanetary shocks: effect on spectral steepening*, in *37th International Cosmic Ray Conference. 12-23 July 2021. Berlin*, p. 1358, Mar., 2022.

[8] J.W. Armstrong, B.J. Rickett and S.R. Spangler, *Electron density power spectrum in the local interstellar medium*, **443** (1995) 209.

[9] Y. Hobara, M. Balikhin, V. Krasnoselskikh, M. Gedalin and H. Yamagishi, *Statistical study of the quasi-perpendicular shock ramp widths*, *Journal of Geophysical Research: Space Physics* **115** (2010) A11106 [https://agupubs.onlinelibrary.wiley.com/doi/pdf/10.1029/2010JA015659].